Aquatic Mammals 2019, *45*(6), 717-732, DOI 10.1578/AM.45.6.2019.717

The Role of Material Properties in Cetacean Hearing Models: Knowns and Unknowns

Andrew A. Tubelli[1] and Darlene R. Ketten[1, 2]

[1]*Boston University Hearing Research Center and Department of Biomedical Engineering, 44 Cummington Mall, Boston, MA 02215, USA*
E-mail: atubelli@bu.edu
[2]*Biology Department, Woods Hole Oceanographic Institution, 266 Woods Hole Road, Woods Hole, MA 02543, USA*

Abstract

Computational, anatomically derived modeling of hearing in mysticetes (baleen whales) can be a valuable technique for estimating hearing ranges when live animal experimental measures are not possible. To date, the authors have produced finite element models (FEMs) for the middle ears of two baleen whales. These models provide an analysis of the middle-ear transfer function that is the basis for estimating best hearing range and auditory thresholds of any mammal. One difficulty in modeling whale hearing is that mechanical and physical tissue properties required for these models have not been measured in many cetaceans, and those that have been measured show significant species differences. Therefore, we undertook a study to examine how varying tissue properties over a wide potential range based on known values of mammalian tissue analogues affect the model output and estimated hearing ranges in the humpback whale (*Megaptera novaeangliae*). Twenty-one total parametric variations were tested. Model results indicate that eight parameters can have significant impacts on hearing estimates, affecting key hearing characteristics, including peak frequency, auditory bandwidth, low- and high-cutoff frequencies, and response magnitude.

Key Words: humpback whale, *Megaptera novaeangliae*, cetacean, hearing, model, material properties, mechanics

Introduction

No current method of live animal measurements of audiograms, either behaviorally or through brainstem responses, is feasible for any baleen whale. By contrast, inner- and middle-ear models are well-established approaches to determine hearing in terrestrial mammals, and the same methods are practical to use for any species of toothed and baleen whale (Odontoceti and Mysticeti, respectively) for which anatomical information exists.

As part of an ongoing research project on comprehensive modeling of cetacean hearing, we have previously completed finite element models (FEMs) of the middle ear for two baleen whale species: minke (*Balaenoptera acutorostrata*) and humpback (*Megaptera novaeangliae*) (Tubelli et al., 2012, 2018). Audiograms are the result of the collective responses of the three major partitions of the ear (external, middle, and inner) for which the middle-ear transfer function, a measure of stapes velocity relative to acoustic pressure at any proposed input to the middle ear, is responsible for describing the bandwidth of hearing (Dallos, 1973; Rosowski, 1991; Ruggero & Temchin, 2002).

Most computational models oblige us to make assumptions for some input parameters for which material properties are unknown. Although approximations can be made based on similar tissue characteristics, these models provide the most useful insight when we replace assumptions with species-specific, measured tissue data. Therefore, the effectiveness of computationally modeling mysticete hearing thresholds critically depends on the values of chosen input parameters—that is, selection of material and mechanical properties that are as close to *in vivo* values as possible. One difficulty with models for whale ears is that the majority of material properties of key structures have not been measured for most cetaceans, both mysticetes and odontocetes alike. Further, those that have been measured show significant species differences, indicating that one value is not appropriate for all species models (Nummela et al., 1999; Tubelli et al., 2014; Schmidt et al., 2018). There is concern therefore that models employing arbitrary surrogate material property values without explanation of selection criteria may not provide accurate model results. In the absence of actual physical and mechanical property measurements, middle-ear parameters can be estimated based on measured values from similar tissues in

terrestrial mammals. These surrogate values should also be informed by an understanding of how differences in multiple material property values affect model outputs and may be further refined through model parameter tuning.

The goal of the present study is to assess which input parameters are most critical and to enumerate those that currently lack experimental measures by studying sensitivity of the transfer function of finite element middle-ear models to those input parameters using the humpback whale as an example species. Parameters for our studies were based on the structural similarity of multiple measured mammalian tissue analogues. Ranges of values were selected for parametric analysis to understand the effects of varying each parameter on the model output. We employed model parametric sensitivity analysis, which is a method of individually changing input parameter values and assessing the resulting variation in output. This technique is useful for quantifying parameter uncertainty. In the case of cetacean hearing models, for which so many material and mechanical properties have no experimental measures, sensitivity analysis is critical. These methods, coupled with the middle-ear geometry and cytoarchitecture extracted from imaging and histology, provide a methodology to more accurately estimate hearing of any cetacean species or, in fact, of any species untestable by conventional techniques.

Previous publications (Tubelli et al., 2012, 2018) touched on a few of the properties that are thought to be most important in hearing. This article provides a more comprehensive discussion of 21 input parameters and their effects on the middle-ear transfer function in the humpback whale. Because of the diversity of researchers and regulators concerned with marine mammal hearing studies, we provide herein both a comprehensible introduction to the modeling process and technical information from this study in a way that can be appreciated by those differing technical backgrounds.

Methods

The anatomy and parameters for the humpback whale model were taken directly from Tubelli et al. (2018). Briefly, the middle ear is surrounded by the tympanic bulla, a shell-like bony case containing the primary functional elements of the middle ear: the eardrum or tympanic membrane; the "ossicular chain," a jointed three-bone (malleus, incus, and stapes) middle-ear lever system that connects the eardrum via the malleus through the incus to the stapes that is attached to the oval window (the entry to the inner ear); and associated ligaments and tendons that provide tension and support for the ossicles.

In this study, anatomical data for the humpback bulla and its parts were compiled from CT scans of three similarly sized ears obtained from both male and female stranded animals ranging in age from yearling to adult. Although head sizes change with age, ears from both young and older animals are appropriate for these studies because cetacean ears are precocial, operating in utero, and have been shown to have fully formed middle and inner ears in neonates with auditory responses consistent with adults (Lancaster et al., 2014; Plencner, 2017; Wahlberg et al., 2017). All ears were scanned and imaged from freshly extracted Code 3 (moderately decomposed) stranded specimens at a resolution of 0.1-mm isotropic voxels. Some specimens were also scanned after fixation to verify tissue preservation. To verify tissue dimensions from scans, measurements were performed as well on either histological sections or on frozen-thawed ears. The anatomical structures with the best quality were chosen from each scan dataset for a composite reconstruction. Further details can be found in the original publication (Tubelli et al., 2018).

The middle-ear tissues were segmented from the CT scans and reconstructed with Amira software (Mercury Computer Systems, Chelmsford, MA, USA). These included the tympanic bone, malleus, incus, stapes, incudo-stapedial joint, incudo-malleal joint, annular ligament (a fibrous ring that attaches the stapes to the oval window), and the tympanic membrane (Figure 1A). In mysticetes, the tympanic membrane is a massive and well-developed membrane shaped like a hollow finger of a glove (and therefore commonly referred to as a "glove finger") with a relatively thick ligament that inserts onto the malleus (Lillie, 1910; Fraser & Purves, 1960; Ketten, 2000). Additionally, the stapedius muscle tendon and posterior incudal ligament were reconstructed from anatomical landmarks with the consistency of position and dimensions compared and confirmed via gross dissection and histological sections of other specimen ears of the same species. The models were secondarily "topologized"—that is, surface shapes were redefined in terms of a mesh of adjoined triangular elements—in Maya software (Autodesk Inc., San Rafael, CA, USA) to provide a best fit of the heavily contoured geometry of the middle-ear structures. The finalized geometry of the humpback whale reconstruction contained 26,615 triangular surface elements (Figure 1B & C).

Because our main goal was to look primarily at alterations in response values, we opted to test middle-ear response variations based on a single pressure input at a commonly configured point on the tympanic bone in the humpback model rather than compare values from tympanic membrane inputs for simplicity. Fixed boundary conditions were set at the connecting regions of the tympanic bone to the periotic bone as well as the rim of the annular ligament distal from the stapes to simulate

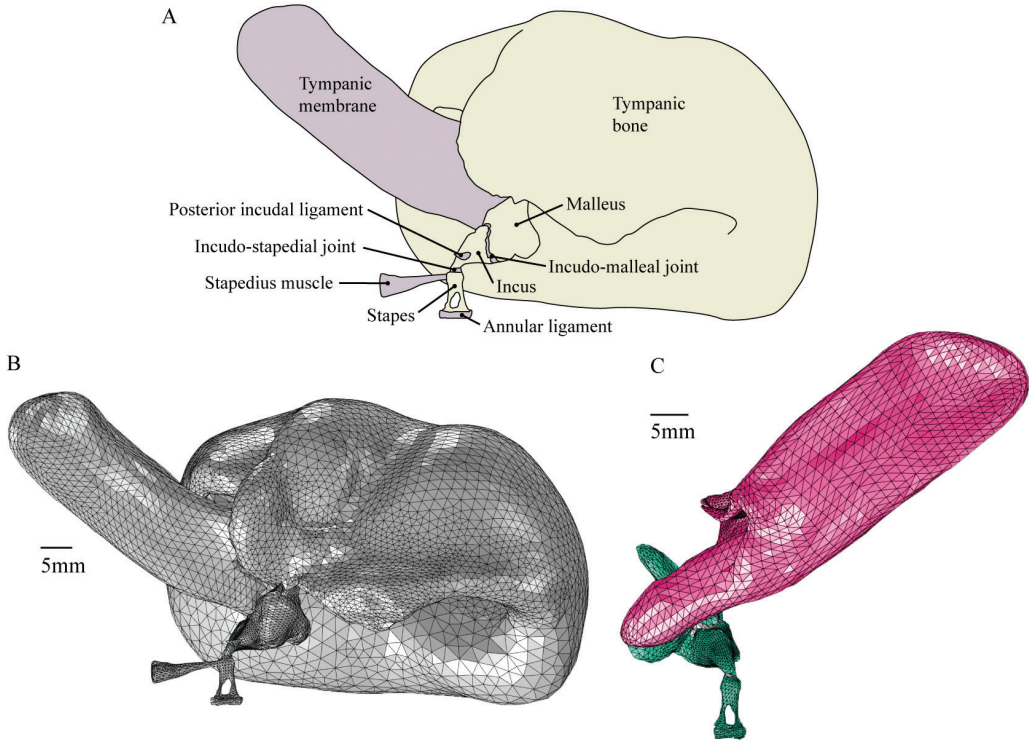

Figure 1. (A) Labeled components of the humpback whale (*Megaptera novaeangliae*) model from a lateral view, (B) mesh geometry for humpback whale from a lateral view, and (C) comparison of geometry of the tympanic membrane (magenta) relative to ossicles (teal) from a medial view

differential motion of the stapes with respect to the periotic bone since this is what translates to cochlear fluid motion and, subsequently, the sensation of hearing, as is known in all mammals.

Study Parameters

Each input parameter in the model was given a primary value and varied individually in a series of parametric sweeps within a wide range to include related physiological values measured in other mammalian tissues (Table 1). Details for sources of values used for each parameter are given below.

Elastic Modulus—The elastic modulus of a material is the relation between force on a material and its resulting deformation. Stiffer materials will have higher elastic moduli—that is, high force can be exerted on stiffer materials with less resultant deformation. Cetacean bullae and middle-ear bones are known to be highly mineralized with some of the highest known modulus values for bone (Currey, 1979; Lees et al., 1996; Zioupos et al., 2000; Zioupos, 2005; Tubelli et al., 2014; Schmidt et al., 2018). For example, Tubelli et al. (2014) found that the elastic moduli of ossicles in the measured mysticete species are 35 GPa, on average. Odontocetes have significantly stiffer middle-ear components with an even higher ossicular elastic moduli of ~60 GPa, on average. In comparison, some terrestrial mammals have ossicular elastic moduli of less than 20 GPa (Speirs et al., 1999; Soons et al., 2010).

For the humpback whale, the mean elastic modulus value for mysticetes from Tubelli et al. (2014) was used for a primary value. Although values measured in each of the studies investigating cetacean ear bone elastic moduli converge on similar results, sensitivity analysis was performed between 10 MPa to 100 GPa to study the general effect this property has on the transfer function.

The variations in anatomy and material properties of each of the middle-ear bones, their joint structures, and their associated soft tissues (muscle tendons and ligaments) are all critical to accurate modeling. Soft tissues come in many varieties (e.g., fat, muscle, and ligaments) and, therefore, have a wide range of possible material property values. Thus, soft tissues in the model were divided into four groups: (1) articular soft tissue

Table 1. Primary, low, and high values for each parameter used in the model. * = directly measured for humpback whales (*Megaptera novaeangliae*), † = extrapolated from cetacean values, ‡ = extrapolated from terrestrial values, and § = estimated.

Parameter	Low value	Primary value	High value
Elastic modulus, bone (Pa)	1×10^{8}	3.5×10^{10}†	1×10^{11}
Elastic modulus, tympanic membrane (Pa)	1×10^{4}	1.35×10^{7}‡	1×10^{10}
Elastic modulus, annular ligament (Pa)	1×10^{4}	2.9×10^{5}‡	1×10^{10}
Elastic modulus, articular soft tissue (Pa)	1×10^{4}	1×10^{7}‡	1×10^{10}
Elastic modulus, suspensory soft tissue (Pa)	1×10^{4}	1×10^{7}‡	1×10^{10}
Density, bone (kg/m^3)	1×10^{3}	2.3×10^{3}*	5×10^{3}
Density, tympanic membrane (kg/m^3)	1×10^{3}	1.32×10^{3}‡	5×10^{3}
Density, annular ligament (kg/m^3)	1×10^{3}	1.32×10^{3}‡	5×10^{3}
Density, articular soft tissue (kg/m^3)	1×10^{3}	1.32×10^{3}‡	5×10^{3}
Density, suspensory soft tissue (kg/m^3)	1×10^{3}	1.32×10^{3}‡	5×10^{3}
Poisson's ratio, bone	-0.49	0.3§	0.45
Poisson's ratio, tympanic membrane	-0.49	0.45§	0.45
Poisson's ratio, annular ligament	-0.49	0.45§	0.45
Poisson's ratio, articular soft tissue	-0.49	0.45§	0.45
Poisson's ratio, suspensory soft tissue	-0.49	0.45§	0.45
Cochlear damping constant (N s/m)	0	0.217‡	1
Rayleigh damping mass coefficient (s^{-1})	0	1×10^{3}§	1×10^{3}
Rayleigh damping stiffness coefficient (s)	0	1×10^{-5}§	1
Isotropic loss factor, all tissues	0	--§	1
Isotropic loss factor, bone	0	--§	1
Isotropic loss factor, soft tissue	0	--§	1

(incudo-stapedial joint and incudo-malleal joint), (2) annular ligament, (3) tympanic membrane, and (4) suspensory soft tissues (posterior incudal ligament and stapedial muscle tendon). The tensor tympani tendon is typically seen in mammals, though it was not included in the humpback model since it was not present in dissected ear samples. It is unknown whether it is absent in this species or rapidly degraded *postmortem*. Elastic moduli measurements have been published on some head tissues in one odontocete, a previously frozen beaked whale specimen (Soldevilla et al., 2005), but there are no published measurements for cetacean middle- or inner-ear soft tissues. Articular and suspensory soft tissues were given a primary elastic modulus value of 10 MPa, the general order of magnitude of experimentally measured values for ligaments and tendons of terrestrial animals (McGough et al., 1996; Stäubli et al., 1999; Provenzano et al., 2002; Hashemi et al., 2005; Chandrashekar et al., 2006). The annular ligament was given a primary value of 0.29 MPa, a mean of the values used in other mammalian middle-ear modeling studies (Koike et al., 2002; Homma et al., 2010; Wang & Gan, 2016; De Greef et al., 2017). Finally, the elastic modulus of the tympanic membrane was assigned 13.5 MPa, an average value of the pars flaccida, a portion of the tympanic membrane most similar to the glove finger structure according to Fraser & Purves (1954), which has been used in other terrestrial mammalian middle-ear FEMs and ranged from 7 to 20 MPa. Sensitivity analysis was performed between 10 kPa to 10 GPa for all soft tissue groups.

Density—The primary parameter value for ear bone density used in the model is 2.30×10^{3} kg/m^3, taken as the mean value of densities for humpback whale ossicles measured by Nummela et al. (1999). Sensitivity analysis values ranged from 1×10^{3} kg/m^3 to 5×10^{3} kg/m^3.

Soft tissue densities are unknown for cetaceans with the exception of fats (Soldevilla et al., 2005; Yamato et al., 2012), but density data are available for tendons in terrestrial mammalian species (Ker, 1981; Kuo et al., 2001; Hashemi et al., 2005).

Densities of all soft tissues in the models were set as 1.32×10^3 kg/m^3, the mean of the measured values from three terrestrial mammalian tendon density sources that is also similar to values of soft tissue densities used in other middle-ear models (Koike et al., 2002; Gan et al., 2004; Homma et al., 2009; Wang & Gan, 2016). The range of values used for sensitivity analysis for all soft tissues was the same as that used for bone.

Poisson's Ratio—Poisson's ratio is a means of quantifying how a material alters shape when compressed or stretched. Technically, it is the ratio of deformations perpendicular to a uniaxial compressive force or transverse to the direction of stretch. The possible range of values for *isotropic* materials (i.e., when a material property measures the same in all directions) spans -1 to 0.5, where 0.5 is incompressible vs those with negative values that are *auxetic* materials (i.e., materials that shrink in all directions when compressed). Values greater than 0.5 are possible for *anisotropic* materials. Published middle-ear models almost invariably use 0.3 for bone and 0.3 to 0.45 for soft tissues (e.g., Gan et al., 2004; Tuck-Lee et al., 2008; Homma et al., 2010).

Here, soft tissue was set as 0.45. Measured values of Poisson's ratio in bone have a wider range than is reflected in models—between 0.07 to > 0.5 (McElhaney, 1966; Reilly & Burstein, 1975; Dalstra et al., 1993; Shahar et al., 2007). Tendons have a wide range of Poisson's ratios, with some studies obtaining positive values of approximately 0.1 to 4 (Lynch et al., 2003; Vergari et al., 2011; Chernak & Thelen, 2012; Thorpe et al., 2013, 2014), whereas other studies report negative values approaching -10 (Gatt et al., 2015). The current study used isotropic materials for simplicity, thus values in the simulation were kept within a permissible range to satisfy equations for linear elastic materials. Values between -0.49 and 0.4 were tested with sensitivity analysis. Values close to the upper limit of Poisson's ratio for linear materials (0.5) in FEMs are known to give inaccurate results; for technical reasons, see Bathe (2006). For this reason, values greater than the primary value of 0.45 were avoided.

Damping—Damping is a form of energy dissipation from a system over time. There are many different types of damping, three of which are included in the middle-ear models: (1) cochlear damping, (2) Rayleigh damping, and (3) isotropic damping. *Cochlear damping* is attributed to the fluid of the cochlea reacting to the stapes footplate velocity. The cochlear damping constant can be derived from the measurements of several terrestrial mammalian species, ranging from 0.059 to 0.891 N s/m (Møller, 1965; Lynch et al., 1982; Merchant et al., 1996; Aibara et al., 2001; Puria, 2003; Slama et al., 2010). This value is species-dependent and assumes a constant cochlear input impedance. The primary value, 0.217 N s/m, was chosen from Aibara et al. (2001) but tested between 0 and 1 with parametric sensitivity analysis.

Rayleigh damping is a classical type of structural damping used in many modeling studies that provides a simplified approximation of energy dissipation and has been applied to middle-ear models (Ferris & Prendergast, 2000; Koike et al., 2002; Wang & Gan, 2016; De Greef et al., 2017). Here, it was used for primary models. It consists of two parameters: (1) a mass coefficient α and (2) a stiffness coefficient β. In previous middle-ear FEMs, α was set to either 0 s^{-1} or 260 s^{-1} and β between 1.86×10^{-5} s and 5×10^{-4} s (Ferris & Prendergast, 2000; Koike et al., 2002; Gan et al., 2004; Hoffstetter et al., 2010; Wang & Gan, 2016; De Greef et al., 2017). This model employed primary values of 1×10^3 s^{-1} for α and 1×10^{-5} for β.

Rayleigh damping may not be an optimal representation of damping in the middle ear since structures can become overdamped at high frequencies (Zhang & Gan, 2013); therefore, *isotropic damping*, characterized by isotropic loss factors, was tested as an alternative. Three parametric sweeps employing isotropic damping were performed: (1) bone damping only, (2) soft tissue damping only, and (3) both bone and soft tissue damping. Primary values did not contain isotropic damping; values between 0 and 1 were investigated in sensitivity analysis. Both Rayleigh and isotropic damping were separately investigated as opposing types of damping; cochlear damping was included in all cases.

The FEMs were designed to be linear for simplicity and solved with COMSOL Multiphysics software (COMSOL Inc., Stockholm, Sweden). The output of the models was a series of transfer functions of output velocity at the center of the stapes footplate relative to the input pressure as a function of frequency (1 Hz to 100 kHz). The primary values provided a reference transfer function for each species that was compared with the transfer functions resulting from all parameter changes.

Results

Parameters that when changed produce a significant effect on the response and therefore transfer function, here defined as any change greater than 6 dB from the primary transfer functions, are presented in Figure 2. More details about those effects on frequency and magnitude are given in the subsequent text and figures.

Elastic Modulus

All tested changes to bone and soft tissue elastic moduli resulted in significant changes in the transfer function. For bone, increases in the elastic modulus had the effect of shifting the transfer function higher in frequency (Figure 3). Changing the tympanic membrane elastic modulus only resulted in significant changes in the mid-frequency region (i.e., the peak region) (Figure 4). Increasing the tympanic membrane elastic modulus primarily introduced resonances around the peak frequency. The annular ligament elastic modulus affected the transfer function most strongly in magnitude; the peak frequency and bandwidth also showed slight shifts (Figure 5). A higher elastic modulus of the annular ligament resulted in a lower magnitude.

Increasing the elastic modulus of articular soft tissues (the highest values of which simulate a rigid joint tissue between the ossicles) both increased magnitude of the transfer function and shifted the peak to higher frequencies (Figure 6). Additionally, at higher elastic moduli values, when the joints are most rigid, the high-frequency roll-off became shallower. Increasing suspensory soft tissue elastic moduli primarily affected dampening of the low and mid frequencies (Figure 7). The magnitude at high frequencies slightly increased as well.

Density

Density of bone, when increased, affects the transfer function by shifting the peak and high-frequency slope downward in frequency (Figure 8). Lower frequencies (less than 1 kHz) are unaffected. Changing densities of the tympanic membrane, annular ligament, articular soft tissues, and suspensory soft tissues have no significant effect on the transfer function.

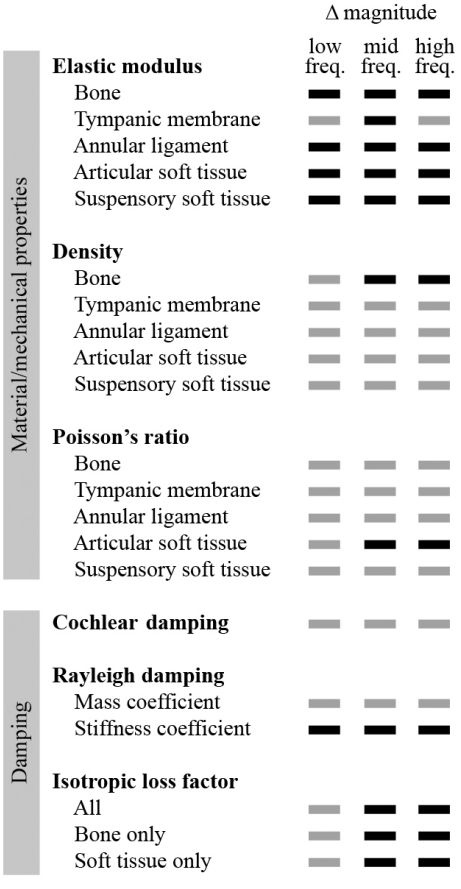

Figure 2. Summary of the effects of parameter changes, both material/mechanical properties and damping, on the transfer functions of humpback whales with respect to magnitude. Values highlighted in black are those that showed a significant difference (i.e., a change of ±6 dB) from the primary transfer functions of each species, split into low-, mid- (peak), and high-frequency regions.

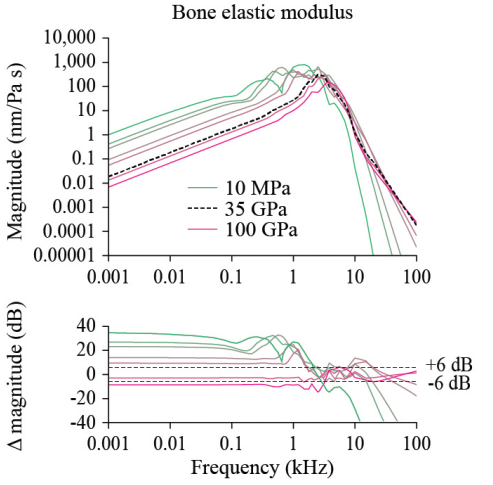

Figure 3. The effects of changing bone elastic modulus on the transfer functions of humpback whales. Top graph shows all transfer function curves for each parameter value (n = 7) compared to the primary transfer function (dotted line). Bottom graph shows the change in magnitude as a function of frequency in dB for which the threshold of significance is defined here as ±6 dB from the primary magnitude. Changes greater than 40 dB are not shown. A color gradient from green to magenta is used to indicate the range of values tested from low to high, respectively. Lowest and highest sensitivity values are labeled in the legend as well as the primary value.

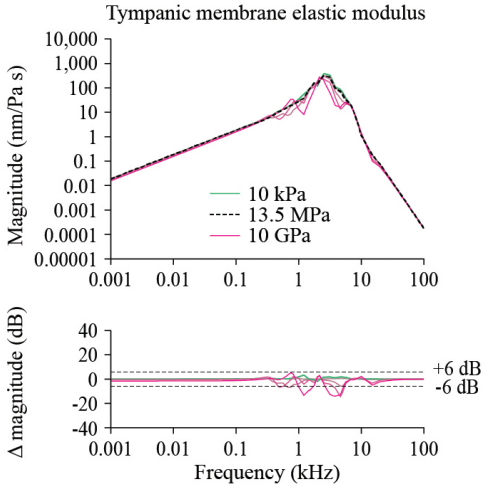

Figure 4. The effects of changing tympanic membrane elastic modulus on the transfer functions of humpback whales. Top graph shows all transfer function curves for each parameter value (n = 7) compared to the primary transfer function (dotted line). Bottom graph shows the change in magnitude as a function of frequency in dB for which the threshold of significance is defined here as ±6 dB from the primary magnitude. A color gradient from green to magenta is used to indicate the range of values tested from low to high, respectively. Lowest and highest sensitivity values are labeled in the legend as well as the primary value.

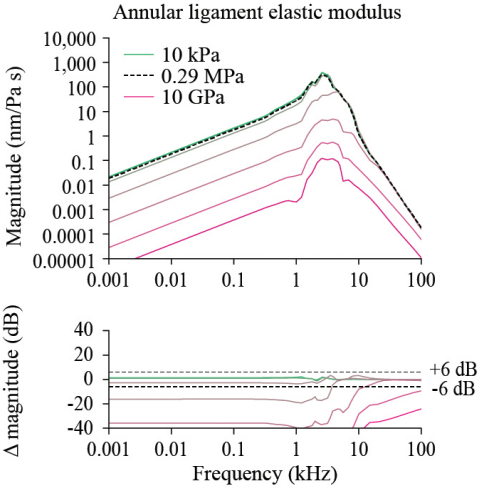

Figure 5. The effects of changing annular ligament elastic modulus on the transfer functions of humpback whales. Top graph shows all transfer function curves for each parameter value (n = 7) compared to the primary transfer function (dotted line). Bottom graph shows the change in magnitude as a function of frequency in dB for which the threshold of significance is defined here as ±6 dB from the primary magnitude. Changes greater than 40 dB are not shown. A color gradient from green to magenta is used to indicate the range of values tested from low to high, respectively. Lowest and highest sensitivity values are labeled in the legend as well as the primary value.

Poisson's Ratio

Poisson's ratio of articular soft tissue has a slight effect on the shape of the transfer function curve, significantly affecting mid and high frequencies (Figure 9). Poisson's ratio of bone, the tympanic membrane, annular ligament, and suspensory soft tissue all have an insignificant effect on the transfer function.

Damping

Changes in the cochlear damping constant exclusively affect the peak frequency region of the transfer function, although insignificantly. The Rayleigh damping stiffness parameter strongly affects the shape of the transfer function. Increased damping results in a smoother transfer function that additionally flattens out the peak (Figure 10). A higher mass damping coefficient smooths the resonances of the transfer function shape (or, rather, a lower mass damping coefficient introduces resonances to the transfer function shape), but this change is not significant.

Higher isotropic damping has greater effects on the mid and high frequencies when damping is modeled with isotropic loss factors rather than Rayleigh damping (Figure 11). The transfer function becomes much smoother with higher damping applied to all tissues together. In all other cases, for lower damping or damping on bone only (Figure 12) or soft tissue only (Figure 13), the transfer function shows several resonances.

From the sensitivity analyses of the middle-ear model, there emerge eight material properties with the highest priorities for obtaining experimental measures for improving middle-ear model accuracy and, subsequently, hearing range estimation. The order of importance based on effects on the transfer function are as follows: (1) Rayleigh damping stiffness coefficient, (2) elastic modulus of articular soft tissue, (3) isotropic loss factor of soft tissue, (4) isotropic loss factor of bone, (5) elastic modulus of annular ligament, (6) elastic modulus of suspensory soft tissue, (7) Poisson's ratio of articular soft tissue, and (8) elastic modulus of tympanic membrane. Figure 14 displays these results in the context of best hearing range estimation (here defined as -40 dB from the peak magnitude). Box plots for the peak frequency, low-frequency cutoff at -40 dB, and high-frequency cutoff at -40 dB show the most probable estimated ranges for each of the most sensitive parameters. The Rayleigh damping stiffness

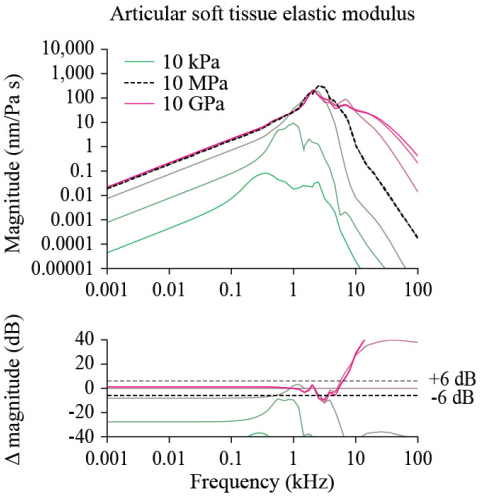

Figure 6. The effects of changing articular soft tissue elastic modulus on the transfer functions of humpback whales. Top graph shows all transfer function curves for each parameter value (n = 7) compared to the primary transfer function (dotted line). Bottom graph shows the change in magnitude as a function of frequency in dB for which the threshold of significance is defined here as ±6 dB from the primary magnitude. Changes greater than 40 dB are not shown. A color gradient from green to magenta is used to indicate the range of values tested from low to high, respectively. Lowest and highest sensitivity values are labeled in the legend as well as the primary value.

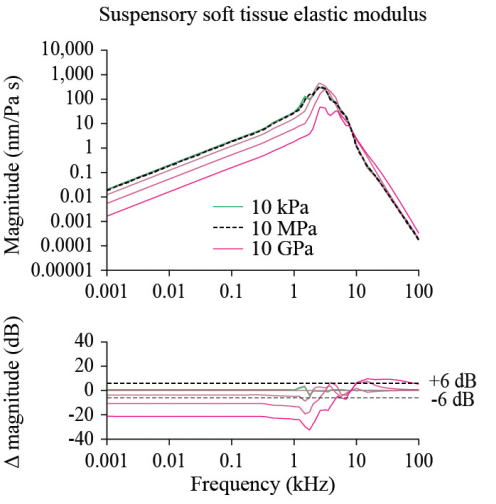

Figure 7. The effects of changing suspensory soft tissue elastic modulus on the transfer functions of humpback whales. Top graph shows all transfer function curves for each parameter value (n = 7) compared to the primary transfer function (dotted line). Bottom graph shows the change in magnitude as a function of frequency in dB for which the threshold of significance is defined here as ±6 dB from the primary magnitude. A color gradient from green to magenta is used to indicate the range of values tested from low to high, respectively. Lowest and highest sensitivity values are labeled in the legend as well as the primary value.

parameter β gives the most extreme result, but if we consider that isotropic damping gives a closer approximation to the audiogram, we can ignore this parameter. The most probable ranges for the peak frequency (defined here as the range between the lowest value of the first quartile to the highest value of the third quartile for the peak boxplots in Figure 14, excluding β) are between 2 and 4 kHz for the humpback whale. The widest bandwidth of hearing (defined as the lowest value of the first quartile of the low-frequency box plots to the highest value of the third quartile of the high-frequency box plots in Figure 14, excluding β) for the humpback whale is likely between 50 Hz to 20 kHz.

Discussion

While parameters were given wide ranges of values during sensitivity analysis, it was expected that only a subset of values in each range would be physiologically relevant. A potentially more accurate range can be estimated from values already measured in literature, and many primary values in the models were chosen this way. It must be noted, however, that because most properties of cetacean tissue remain unknown, it is entirely possible that the real values may be outside the standard range of values of terrestrial mammals. For example, the ear bones of cetaceans have unusually high mineralization and a greater percentage of the bullar capsule comprised of exceedingly dense compact bone as compared to ear bones in any other known mammal or even other cetacean bone (Currey, 1979; Kim et al., 2014; Tubelli et al., 2014; Schmidt et al., 2018). This implies that an unusually high elastic modulus is appropriate. It has been suggested that this is an adaptation related to diving as well as having consequences for underwater hearing (Currey, 1979; Kim et al., 2014; Tubelli et al., 2014; Schmidt et al., 2018). Other yet unmeasured tissue parameters could similarly diverge considerably from terrestrial tissue values based on anatomy evolved to be uniquely marine.

In the case of elastic moduli and densities of ear bones, measurements have been made for a few cetacean species (Currey, 1979; Nummela et al., 1999; Kim et al., 2014; Tubelli et al., 2014; Schmidt et al., 2018) and, thus, sensitivity analysis was purely an exercise in understanding the role of these parameters in shaping the

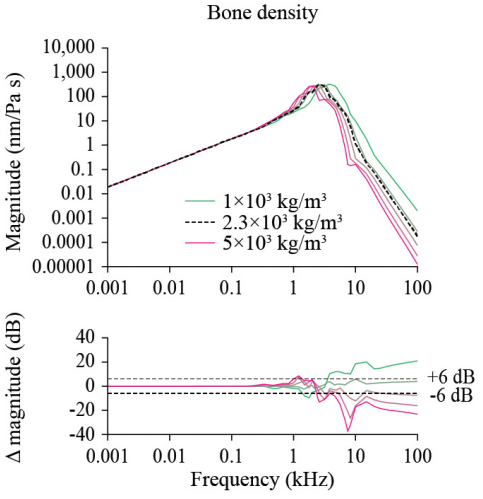

Figure 8. The effects of changing bone density on the transfer functions of humpback whales. Top graph shows all transfer function curves for each parameter value (n = 7) compared to the primary transfer function (dotted line). Bottom graph shows the change in magnitude as a function of frequency in dB for which the threshold of significance is defined here as ±6 dB from the primary magnitude. A color gradient from green to magenta is used to indicate the range of values tested from low to high, respectively. Lowest and highest sensitivity values are labeled in the legend as well as the primary value.

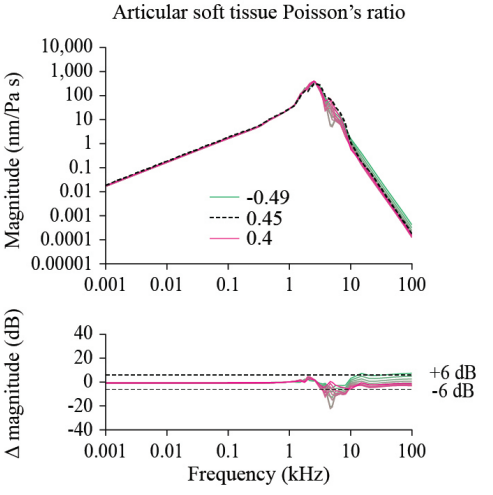

Figure 9. The effects of changing articular soft tissue Poisson's ratio on the transfer functions of humpback whales. Top graph shows all transfer function curves for each parameter value (n = 11) compared to the primary transfer function (dotted line). Bottom graph shows the change in magnitude as a function of frequency in dB for which the threshold of significance is defined here as ±6 dB from the primary magnitude. A color gradient from green to magenta is used to indicate the range of values tested from low to high, respectively. Lowest and highest sensitivity values are labeled in the legend as well as the primary value.

transfer function. The effects of changing bone elastic moduli (Figure 3), for which a higher elastic modulus results in a higher frequency peak, is reasonable given measurements performed by Tubelli et al. (2014), as well as those by Schmidt et al. (2018) that showed that odontocetes have higher ossicular elastic moduli than mysticetes. Mysticetes are generally categorized as lower frequency animals and, thus, it is consistent that the bones are less stiff than in odontocetes.

Changes in bone density affecting only the mid and high frequencies of the transfer functions also make sense when considering the model in the context of two properties: (1) mass and (2) stiffness. These two properties are the most important components in determining the natural frequency (i.e., the most sensitive frequency) of a system and are related by

$$f_n = \frac{1}{2\pi}\sqrt{\frac{k}{m}} \qquad \text{(Equation 1)}$$

where f_n is natural frequency, k is stiffness, and m is mass. As shown in Equation 1, mass is inversely proportional to the natural frequency. A more massive ear favors a lower resonant frequency. In the opposite manner, stiffness is proportional to natural frequency; thus, a stiffer middle ear favors a higher resonant frequency. This relation is a lumped-element simplification of the middle-ear system that generally explains why mysticetes, with their more massive ossicles in comparison to odontocetes, would be more sensitive at lower frequencies (Fleischer, 1978; Wartzok & Ketten, 1999). Density is a property that depends on mass; therefore, we would expect lower frequencies to be less inhibited, whereas higher frequencies would be significantly attenuated in denser ears due to mass domination at those frequencies.

The stapes complex (i.e., the stapes and annular ligament) can be considered a mass-spring system, with the stapes as the mass and the annular ligament as the spring supplying the stiffness (Fleischer, 1978). Together, they transfer the mechanical energy of the middle ear to fluid motion in the cochlea via piston-like motion of the stapes (Høgmoen & Gundersen, 1977; Rosowski, 1994). Where mass can attenuate vibration at higher frequencies (as seen in the response of the transfer function to changes in density in Figure 8), stiffness likewise can attenuate the low-frequency response. In support of this, Figure 5 shows that within the range of parametric values

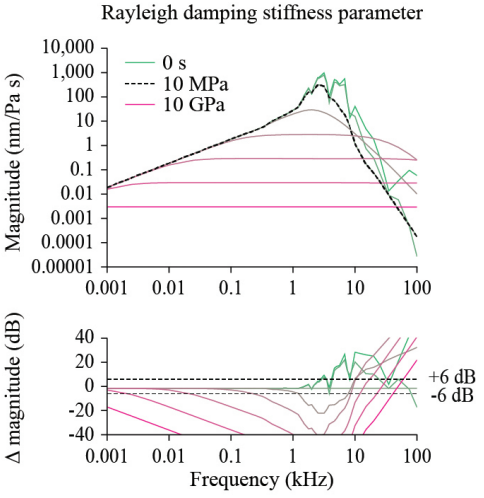

Figure 10. The effects of changing Rayleigh damping stiffness parameter on the transfer functions of humpback whales. Top graph shows all transfer function curves for each parameter value (n = 8) compared to the primary transfer function (dotted line). Bottom graph shows the change in magnitude as a function of frequency in dB for which the threshold of significance is defined here as ±6 dB from the primary magnitude. Changes greater than 40 dB are not shown. A color gradient from green to magenta is used to indicate the range of values tested from low to high, respectively. Lowest and highest sensitivity values are labeled in the legend as well as the primary value.

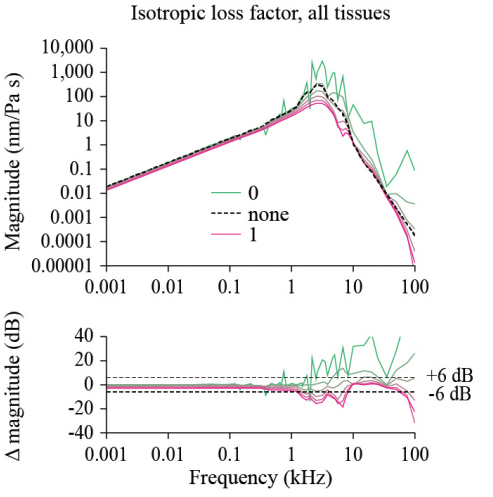

Figure 11. The effects of adding isotropic damping on all tissues, replacing Rayleigh damping, on the transfer functions of humpback whales. Top graph shows all transfer function curves for each parameter value (n = 6) compared to the primary transfer function (dotted line). Bottom graph shows the change in magnitude as a function of frequency in dB for which the threshold of significance is defined here as ±6 dB from the primary magnitude. Changes greater than 40 dB are not shown. A color gradient from green to magenta is used to indicate the range of values tested from low to high, respectively. Lowest and highest sensitivity values are labeled in the legend as well as the primary value.

tested, lower frequencies are orders of magnitude more affected by changes in annular ligament elastic moduli than higher frequencies. To a lesser extent, the suspensory soft tissues function much in the same way, with the elastic modulus controlling how tight each of the ligaments and muscle tendons are, or how stiff the system is, and thus affecting the magnitude of the low-frequency response (Figure 7). Additionally, given the orientation of the annular ligament around the footplate of the stapes, anchoring it to the periotic bone, the stiffness of the annular ligament effectively acts to dampen the motion of the stapes, which explains why increasing annular ligament elastic modulus strongly transforms the transfer function lower in magnitude. Sensitivity analysis of the annular ligament and suspensory soft tissue elastic moduli in humans yields results similar to this study (Ferris & Prendergast, 2000; De Greef et al., 2017).

Articular soft tissue in this study is comprised of the interossicular joints: the incudo-malleal joint and the incudo-stapedial joint. Results of parametric studies combine the effects of these tissues; however, there are differences between the tissues and between the two suborders. In many middle-ear models, the incudo-malleal joint is modeled as rigid, with an elastic modulus equal to the bone (Gan et al., 2004; Homma et al., 2009; Hoffstetter et al., 2010). This is backed by some experimental sources in terrestrial mammals (Kirikae, 1960; Gundersen & Høgmoen, 1976) but argued to be more flexible in others (Willi et al., 2002; Nakajima et al., 2009). In whales and dolphins, the ossicles are not fused, and mysticete ossicles are more loosely joined, but there is no consistent comparative quantitative measurement of the properties of interossicular connections in cetaceans (Fleischer, 1978; Ketten, 2000). Parametric analysis results reveal that choosing different parameter values will have a dramatic effect on the shape of the transfer function at all frequencies (Figure 6), and, thus, the mechanical properties should be studied further.

The cochlear damping constant controls the cochlear input impedance, which is the contribution of the cochlear load to the middle-ear response (Rosowski, 1994). In this study, changes in the cochlear damping constant have an insignificant effect on the humpback whale transfer function. De Greef et al. (2017) examined the change

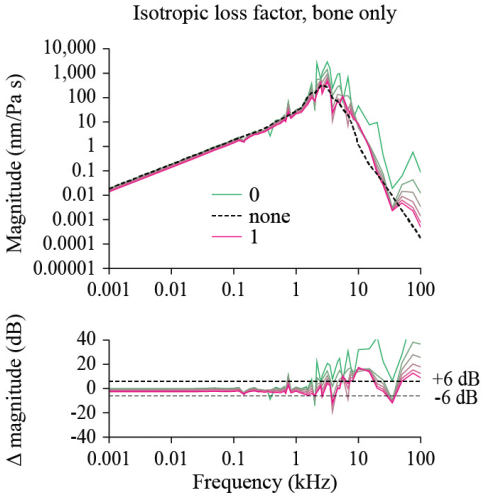

Figure 12. The effects of adding isotropic damping on bone, replacing Rayleigh damping, on the transfer functions of humpback whales. Top graph shows all transfer function curves for each parameter value (n = 6) compared to the primary transfer function (dotted line). Bottom graph shows the change in magnitude as a function of frequency in dB for which the threshold of significance is defined here as ±6 dB from the primary magnitude. Changes greater than 40 dB are not shown. A color gradient from green to magenta is used to indicate the range of values tested from low to high, respectively. Lowest and highest sensitivity values are labeled in the legend as well as the primary value.

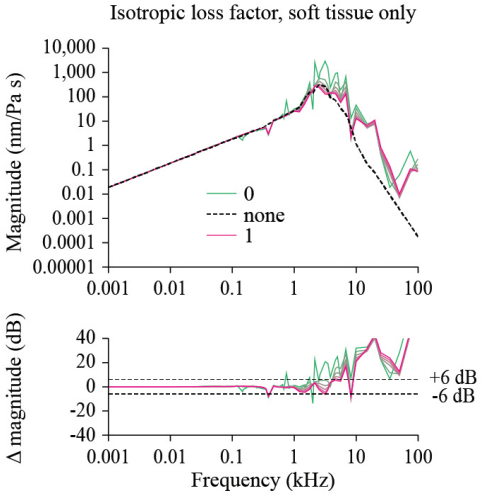

Figure 13. The effects of adding isotropic damping on soft tissues, replacing Rayleigh damping, on the transfer functions of humpback whales. Top graph shows all transfer function curves for each parameter value (n = 6) compared to the primary transfer function (dotted line). Bottom graph shows the change in magnitude as a function of frequency in dB for which the threshold of significance is defined here as ±6 dB from the primary magnitude. A color gradient from green to magenta is used to indicate the range of values tested from low to high, respectively. Lowest and highest sensitivity values are labeled in the legend as well as the primary value.

in the human middle-ear transfer function using cochlear impedance data (rather than a simpler cochlear damping constant extracted from these data for simplicity) from four measured sources. The changes to the transfer function were much more significant, suggesting that the cochlear load should be modeled in a less simple way if experimental data for cetacean cochlear input impedance become available.

This study compares the response of the transfer function to two types of damping on the overall system: (1) Rayleigh damping and (2) isotropic damping. Rayleigh damping is commonly used in modeling and was included in the previously published models of the authors (Tubelli et al., 2012, 2018). However, choosing Rayleigh coefficient parameter values in these studies are conjectured as a result of little experimental justification for which values to choose. In spite of these unknowns, this study shows that both α and β smooth the transfer function with the stiffness parameter β taking this smoothing to an extreme (Figure 10). Funnell et al. (1987) have reported similar results for the sensitivity of an eardrum model, although at a much smaller perturbation range. However, Zhang & Gan (2013) reveal that Rayleigh damping results in high frequencies getting overdamped and suggest using viscoelastic damping instead, which, in the case of the tympanic membrane frequency response, gives greater accuracy to the model. The differences between Rayleigh damping with parameters at the primary values and isotropic damping in this study supports this conclusion (Figures 11-13). The distinction between the two types of damping can become crucial at frequencies greater than 3.8 kHz (Zhang & Gan, 2013) and, therefore, may be significant for mysticetes and potentially even more critical for higher frequency cetaceans, which could be compared with audiometric data. For example, according to the standard bottlenose dolphin (*Tursiops truncatus*) audiogram measured by Johnson (1968), the most sensitive region is between 10 and 100 kHz, with high-frequency roll-off starting at approximately 80 kHz. Most of this peak region from the audiogram may be eliminated in a model transfer function with Rayleigh damping applied; therefore, using isotropic loss factors in lieu of Rayleigh damping should result in a closer approximation of models

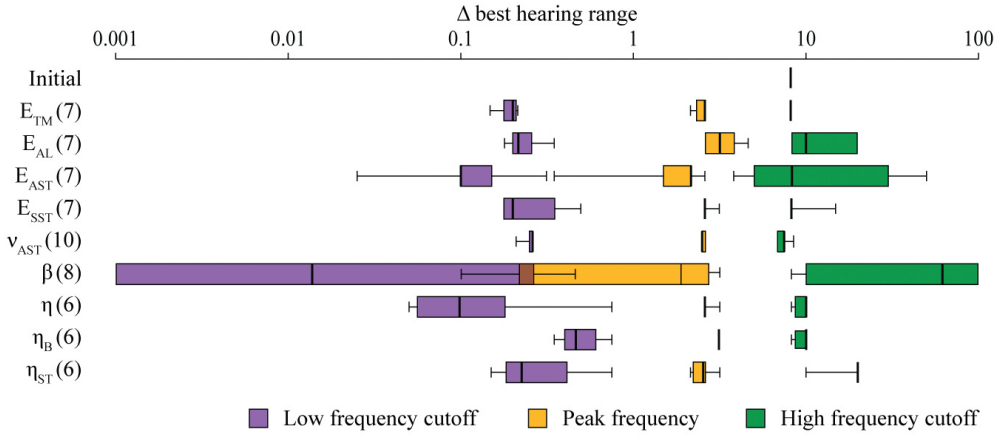

Figure 14. Box plots showing the change in best hearing range at low (purple), peak (orange), and high (green) frequency regions for each change in parameter for each species compared to the primary frequencies. E_{TM} = tympanic membrane elastic modulus, E_{AL} = annular ligament elastic modulus, E_{AST} = articular soft tissue elastic modulus, E_{SST} = suspensory soft tissue elastic modulus, ν_{AST} = articular soft tissue Poisson's ratio, β = Rayleigh damping stiffness coefficient, η = isotropic loss factor for all tissues, η_B = isotropic loss factor for bone, and η_{ST} = isotropic loss factor for soft tissue. The number of data points are shown in parentheses.

to audiograms. A future step is to model loss as a frequency-dependent variable rather than a static value (Homma et al., 2010; Zhang & Gan, 2013).

This model employed input to the tympanic bone for simplicity. It is known that the acoustic fats terminate near the tympanic bone in a number of cetacean species (Norris, 1968; Ketten, 1992, 2000; Yamato et al., 2012); however, the exact terminus can be difficult to determine in *post-mortem* material because of rapid dissolution. In a few extremely fresh odontocete specimens, the acoustic fats have been shown to terminate at the tympanic membrane (Ketten, 2000; Costidis & Rommel, 2012), but the exact location in mysticetes remains unclear. As seen from the transfer functions of the minke (*Balaenoptera acutorostrata*) and humpback whale models from Tubelli et al. (2012, 2018), the tympanic membrane could be the effective input source and the primary, most efficient pathway as is the case for all other mammalian species. For all mysticetes, the hyperdevelopment of a large, well-developed tympanic membrane suggests that this structure is functional. Whether the tympanic membrane of mysticetes (glove finger) maintains the same function as the primary input structure for sound to the middle ear, as in terrestrial mammals, or has evolved to function differently is uncertain. If the tympanic membrane of mysticetes is part of the primary hearing pathway, then having the most accurate related parameters for the membrane has elevated importance in the model. Further investigations with accurate material properties can settle pathway debates and indeed contribute to a better understanding of frequency sensitivities and potential impacts.

It has been demonstrated that combining the separate contributions of the outer, middle, and inner ears together provides a comprehensive, optimal estimation of an audiogram (Ruggero & Temchin, 2002). The pathway to the middle ear is one element but not the most significant for understanding how sound is processed and transferred to the brain. In terms of hearing and audiogram models, the most important elements are not pathways but, rather, the middle-ear transfer function and the inner-ear response maps (Rosowski, 1991, 1994; Ruggero & Temchin, 2002). Total hearing ranges are readily studied through cochlear frequency mapping models, but it is their coupling with middle-ear transfer functions that holds the key to determining peak sensitivities (Dallos, 1973; Rosowski, 1991). The study presented herein looks at the middle-ear component of hearing and is a first step in a complete hearing analysis. In particular, we are addressing the importance of better property measurements, especially for the most sensitive properties (those displayed in Figure 14).

For future studies, both tissue quality and its post-extraction handling are of great importance. It is well established that fixation methods and processing can alter tissue appearance and response characteristics (Schuktnecht, 1993). Just

as fixatives can induce swelling or shrinkage and even decalcify bony tissues, frozen material can lose tissue integrity from several mechanisms if not properly handled—specifically, freezing can induce ice crystal artifacts, and tissues subjected to "frost-free" freezers which have freeze/thaw cycles can have capillary breakdown and suffusion of tissues with bloody residue (Schuknecht, 1993; Meng et al., 2014). The effects of freezing on properties of soft tissues can vary, with some studies reporting no significant changes in mechanical properties for frozen-thawed ligaments and tendons (Woo et al., 1986; Moon et al., 2006), whereas other studies show significant changes (Matthews & Ellis, 1986; Smith et al., 1996; Clavert et al., 2001). However, given the rarity of cetacean material, it is important to employ each specimen within the limits of its use, and it may still be possible to use non-fresh tissue to scientific advantage. As discussed in Tubelli et al. (2018), substandard tissue conditions can be used as experimental reference points that reveal how a degraded structure alters the transfer function. Effects of degraded tissues can be capitalized on by giving the model properties observed in substandard tissues and determining how or if the transfer function is impacted. In this way, we can employ all tissues given a correction factor can be obtained to align the model to experimental data from imperfect material. Acquiring data from more samples with the proper caveats will aid research and may even provide insights into mechanisms for some forms of hearing loss.

Cetacean hearing models can be important tools for estimating the hearing ranges of those species that we cannot measure through behavioral or electrophysiological means. Above all, the accuracy of models depends on input parameters being realistic. Clearly, the parameters that are employed in modeling can produce radically different results depending upon the values chosen. The results of this work focus on changes of single parameters. However, we acknowledge and emphasize that it is important to consider and to investigate the synergistic effects of two or more parametric changes. It is imperative that there be a broader understanding throughout the research community of the potential variations in results given the wide range of tissues employed in modeling studies. It is equally necessary that each study provide some validation of parameters and assessment of how uncertainty regarding those parameters may impact data and interpretations.

Acknowledgments

The authors are grateful to the organizers of the ESOMM 2018 conference for allowing us to participate and present this work, to the Joint Industry Program for Sound in the Sea for funding the present study, and to the Office of Naval Research and the Living Marine Resources Program for their previous support for specimen collection and scanning. Additional support for manuscript preparation and analyses was provided by the Hanse-Wissenschaftskollegg and the Helmholtz Association. We thank Julie Arruda for extensive technical assistance and Dr. H. Steven Colburn, Aleks Zosuls, and Graham Voysey of the Boston University Hearing Research Center for providing advice and comments on the project. We also wish to thank Misty Niemeyer, Kimberly Durham, Katie Moore, Aleta Hohn, and Jennifer Skidmore for their assistance in obtaining specimens as well as the responders and volunteers of the Marine Mammal Health and Stranding Response Program, the International Fund for Animal Welfare (IFAW), and the National Oceanic and Atmospheric Administration (NOAA). Specimens employed in this research were acquired *postmortem* from stranded animals under National Marine Fisheries Service (NMFS) Permit 16591-00 and U.S. Fish and Wildlife Services (USFWS) Permit MA130062-1.

Literature Cited

Aibara, R., Welsh, J. T., Puria, S., & Goode, R. L. (2001). Human middle-ear sound transfer function and cochlear input impedance. *Hearing Research*, *152*(1-2), 100-109. https://doi.org/10.1016/S0378-5955(00)00240-9

Bathe, K. J. (2006). *Finite element procedures*. Englewood Cliffs, NJ: Prentice Hall.

Chandrashekar, N., Mansouri, H., Slauterbeck, J., & Hashemi, J. (2006). Sex-based differences in the tensile properties of the human anterior cruciate ligament. *Journal of Biomechanics*, *39*(16), 2943-2950. https://doi.org/10.1016/j.jbiomech.2005.10.031

Chernak, L. A., & Thelen, D. G. (2012). Tendon motion and strain patterns evaluated with two-dimensional ultrasound elastography. *Journal of Biomechanics*, *45*(15), 2618-2623. https://doi.org/10.1016/j.jbiomech.2012.08.001

Clavert, P., Kempf, J. F., Bonnomet, F., Boutemy, P., Marcelin, L., & Kahn, J. L. (2001). Effects of freezing/thawing on the biomechanical properties of human tendons. *Surgical and Radiologic Anatomy*, *23*(4), 259-262. https://doi.org/10.1007/s00276-001-0259-8

Costidis, A., & Rommel, S. A. (2012). Vascularization of air sinuses and fat bodies in the head of the bottlenose dolphin (*Tursiops truncatus*): Morphological implications on physiology. *Frontiers in Physiology*, *3*, 243. https://doi.org/10.3389/fphys.2012.00243

Currey, J. D. (1979). Mechanical properties of bone tissues with greatly differing functions. *Journal of Biomechanics*, *12*(4), 313-319. https://doi.org/10.1016/0021-9290(79)90073-3

Dallos, P. (1973). *The auditory periphery: Biophysics and physiology*. New York: Academic Press.

Dalstra, M., Huiskes, R., Odgaard, A. V., & Van Erning, L. (1993). Mechanical and textural properties of pelvic trabecular bone. *Journal of Biomechanics*, *26*(4-5), 523-535. https://doi.org/10.1016/0021-9290(93)90014-6

De Greef, D., Pires, F., & Dirckx, J. J. (2017). Effects of model definitions and parameter values in finite element modeling of human middle ear mechanics. *Hearing Research*, *344*, 195-206. https://doi.org/10.1016/j.heares.2016.11.011

Ferris, P., & Prendergast, P. J. (2000). Middle-ear dynamics before and after ossicular replacement. *Journal of Biomechanics*, *33*(5), 581-590. https://doi.org/10.1016/S0021-9290(99)00213-4

Fleischer, G. (1978). Evolutionary principles of the mammalian middle ear. *Advances in Anatomy, Embryology and Cell Biology*, *55*(5), 3-70. https://doi.org/10.1007/978-3-642-67143-2

Fraser, F. C., & Purves, P. E. (1954). Hearing in cetaceans. *Bulletin of the British Museum*, *2*(5), 103-116.

Fraser, F. C., & Purves, P. E. (1960). Anatomy and function of the cetacean ear. *Proceedings of the Royal Society of London B: Biological Sciences*, *152*(946), 62-77. https://doi.org/10.1098/rspb.1960.0024

Funnell, W. R. J., Decraemer, W. F., & Khanna, S. M. (1987). On the damped frequency response of a finite-element model of the cat eardrum. *The Journal of the Acoustical Society of America*, *81*(6), 1851-1859. https://doi.org/10.1121/1.394749

Gan, R. Z., Feng, B., & Sun, Q. (2004). Three-dimensional finite element modeling of human ear for sound transmission. *Annals of Biomedical Engineering*, *32*(6), 847-859. https://doi.org/10.1023/B:ABME.0000030260.22737.53

Gatt, R., Wood, M. V., Gatt, A., Zarb, F., Formosa, C., Azzopardi, K. M., . . . Grima, J. N. (2015). Negative Poisson's ratios in tendons: An unexpected mechanical response. *Acta Biomaterialia*, *24*, 201-208. https://doi.org/10.1016/j.actbio.2015.06.018

Gundersen, T., & Høgmoen, K. (1976). Holographic vibration analysis of the ossicular chain. *Acta Oto-Laryngologica*, *82*(1-6), 16-25. https://doi.org/10.3109/00016487609120858

Hashemi, J., Chandrashekar, N., & Slauterbeck, J. (2005). The mechanical properties of the human patellar tendon are correlated to its mass density and are independent of sex. *Clinical Biomechanics*, *20*(6), 645-652. https://doi.org/10.1016/j.clinbiomech.2005.02.008

Hoffstetter, M., Schardt, F., Lenarz, T., Wacker, S., & Wintermantel, E. (2010). Parameter study on a finite element model of the middle ear. *Biomedical Engineering*, *55*(1), 19-26. https://doi.org/10.1515/bmt.2010.006

Høgmoen, K., & Gundersen, T. (1977). Holographic investigation of stapes footplate movements. *Acta Acustica United with Acustica*, *37*(3), 198-202.

Homma, K., Du, Y., Shimizu, Y., & Puria, S. (2009). Ossicular resonance modes of the human middle ear for bone and air conduction. *The Journal of the Acoustical Society of America*, *125*(2), 968-979. https://doi.org/10.1121/1.3056564

Homma, K., Shimizu, Y., Kim, N., Du, Y., & Puria, S. (2010). Effects of ear-canal pressurization on middle-ear bone- and air-conduction responses. *Hearing Research*, *263*(1-2), 204-215. https://doi.org/10.1016/j.heares.2009.11.013

Johnson, C. S. (1968). Sound detection thresholds in marine mammals. In W. N. Tavolga (Ed.), *Marine bioacoustics* (Vol. 2, pp. 247-260). New York: Pergamon.

Ker, R. F. (1981). Dynamic tensile properties of the plantaris tendon of sheep (*Ovis aries*). *Journal of Experimental Biology*, *93*(1), 283-302.

Ketten, D. R. (1992). The marine mammal ear: Specializations for aquatic audition and echolocation. In D. B. Webster, A. N. Popper, & R. R. Fay (Eds.), *The evolutionary biology of hearing* (pp. 717-750). New York: Springer. https://doi.org/10.1007/978-1-4612-2784-7_44

Ketten, D. R. (2000). Cetacean ears. In W. W. L. Au, A. N. Popper, & R. R. Fay (Eds.), *Hearing by whales and dolphins* (pp. 43-108). New York: Springer. https://doi.org/10.1007/978-1-4612-1150-1_2

Kim, S. L., Thewissen, J. G. M., Churchill, M. M., Suydam, R. S., Ketten, D. R., & Clementz, M. T. (2014). Unique biochemical and mineral composition of whale ear bones. *Physiological and Biochemical Zoology*, *87*(4), 576-584. https://doi.org/10.1086/676309

Kirikae, I. (1960). *The structure and function of the middle ear*. Tokyo: University of Tokyo Press.

Koike, T., Wada, H., & Kobayashi, T. (2002). Modeling of the human middle ear using the finite-element method. *The Journal of the Acoustical Society of America*, *111*(3), 1306-1317. https://doi.org/10.1121/1.1451073

Kuo, P. L., Li, P. C., & Li, M. L. (2001). Elastic properties of tendon measured by two different approaches. *Ultrasound in Medicine & Biology*, *27*(9), 1275-1284. https://doi.org/10.1016/S0301-5629(01)00442-2

Lancaster, W. C., Ary, W. J., Krysl, P., & Cranford, T. W. (2014). Precocial development within the tympanoperiotic complex in cetaceans. *Marine Mammal Science*, *31*(1), 369-375. https://doi.org/10.1111/mms.12145

Lees, S., Hanson, D. B., & Page, E. A. (1996). Some acoustical properties of the otic bones of a fin whale. *The Journal of the Acoustical Society of America*, *99*(4), 2421-2427. https://doi.org/10.1121/1.415430

Lillie, D. G. (1910). Observations on the anatomy and general biology of some members of the larger Cetacea. *Proceedings of the Zoological Society of London*, *80*, 769-792. https://doi.org/10.1111/j.1096-3642.1910.tb01916.x

Lynch, H. A., Johannessen, W., Wu, J. P., Jawa, A., & Elliott, D. M. (2003). Effect of fiber orientation and strain rate on the nonlinear uniaxial tensile material properties of

tendon. *Journal of Biomechanical Engineering*, *125*(5), 726-731. https://doi.org/10.1115/1.1614819

Lynch III, T. J., Nedzelnitsky, V., & Peake, W. T. (1982). Input impedance of the cochlea in cat. *The Journal of the Acoustical Society of America*, *72*(1), 108-130. https://doi.org/10.1121/1.387995

Matthews, L. S., & Ellis, D. (1968). Viscoelastic properties of cat tendon: Effects of time after death and preservation by freezing. *Journal of Biomechanics*, *1*(2), 65-71. https://doi.org/10.1016/0021-9290(68)90008-0

McElhaney, J. H. (1966). Dynamic response of bone and muscle tissue. *Journal of Applied Physiology*, *21*(4), 1231-1236. https://doi.org/10.1152/jappl.1966.21.4.1231

McGough, R. L., Debski, R. E., Taskiran, E., Fu, F. H., & Woo, S. L. (1996). Mechanical properties of the long head of the biceps tendon. *Knee Surgery, Sports Traumatology, Arthroscopy*, *3*(4), 226-229. https://doi.org/10.1007/BF01466622

Meng, H., Janssen, P. M., Grange, R. W., Yang, L., Beggs, A. H., Swanson, L. C., . . . Gussoni, E. (2014). Tissue triage and freezing for models of skeletal muscle disease. *Journal of Visualized Experiments* (*JoVE*), *89*, e51586. https://doi.org/10.3791/51586

Merchant, S. N., Ravicz, M. E., & Rosowski, J. J. (1996). Acoustic input impedance of the stapes and cochlea in human temporal bones. *Hearing Research*, *97*(1-2), 30-45. https://doi.org/10.1016/S0378-5955(96)80005-0

Møller, A. R. (1965). An experimental study of the acoustic impedance of the middle ear and its transmission properties. *Acta Oto-Laryngologica*, *60*(1-6), 129-149. https://doi.org/10.3109/00016486509126996

Moon, D. K., Woo, S. L., Takakura, Y., Gabriel, M. T., & Abramowitch, S. D. (2006). The effects of refreezing on the viscoelastic and tensile properties of ligaments. *Journal of Biomechanics*, *39*(6), 1153-1157. https://doi.org/10.1016/j.jbiomech.2005.02.012

Nakajima, H. H., Dong, W., Olson, E. S., Merchant, S. N., Ravicz, M. E., & Rosowski, J. J. (2009). Differential intracochlear sound pressure measurements in normal human temporal bones. *Journal of the Association for Research in Otolaryngology*, *10*(1), 23. https://doi.org/10.1007/s10162-008-0150-y

Norris, K. S. (1968). The evolution of acoustic mechanisms in odontocete cetaceans. In E. T. Drake (Ed.), *Evolution and environment* (pp. 297-324). New Haven, CT: Yale University Press.

Nummela, S., Wägar, T., Hemilä, S., & Reuter, T. (1999). Scaling of the cetacean middle ear. *Hearing Research*, *133*(1), 71-81. https://doi.org/10.1016/S0378-5955(99)00054-4

Plencner, T. (2017). *Is the hearing of whales and dolphins fully developed at birth? An investigation of the odontocete inner ear* (Unpub. master's thesis). University of Otago, Dunedin, New Zealand.

Provenzano, P. P., Lakes, R. S., Corr, D. T., & Vanderby, R. (2002). Application of nonlinear viscoelastic models to describe ligament behavior. *Biomechanics and Modeling in Mechanobiology*, *1*(1), 45-57. https://doi.org/10.1007/s10237-002-0004-1

Puria, S. (2003). Measurements of human middle ear forward and reverse acoustics: Implications for otoacoustic emissions. *The Journal of the Acoustical Society of America*, *113*(5), 2773-2789. https://doi.org/10.1121/1.1564018

Reilly, D. T., & Burstein, A. H. (1975). The elastic and ultimate properties of compact bone tissue. *Journal of Biomechanics*, *8*(6), 393-405. https://doi.org/10.1016/0021-9290(75)90075-5

Rosowski, J. J. (1991). The effects of external- and middle-ear filtering on auditory threshold and noise-induced hearing loss. *The Journal of the Acoustical Society of America*, *90*(1), 124-135. https://doi.org/10.1121/1.401306

Rosowski, J. J. (1994). Outer and middle ears. In R. R. Fay (Ed.), *Comparative hearing: Mammals* (pp. 172-247). New York: Springer. https://doi.org/10.1007/978-1-4612-2700-7_6

Ruggero, M. A., & Temchin, A. N. (2002). The roles of the external, middle, and inner ears in determining the bandwidth of hearing. *Proceedings of the National Academy of Sciences*, *99*(20), 13206-13210. https://doi.org/10.1073/pnas.202492699

Schmidt, F. N., Delsmann, M. M., Mletzko, K., Yorgan, T. A., Hahn, M., Siebert, U., . . . Rolvien, T. (2018). Ultra-high matrix mineralization of sperm whale auditory ossicles facilitates high sound pressure and high-frequency underwater hearing. *Proceedings of the Royal Society B: Biological Sciences*, *285*(1893), 20181820. https://doi.org/10.1098/rspb.2018.1820

Schuknecht, H. F. (1993). *Pathology of the ear*. Philadelphia, PA: Lea and Febiger.

Shahar, R., Zaslansky, P., Barak, M., Friesem, A. A., Currey, J. D., & Weiner, S. (2007). Anisotropic Poisson's ratio and compression modulus of cortical bone determined by speckle interferometry. *Journal of Biomechanics*, *40*(2), 252-264. https://doi.org/10.1016/j.jbiomech.2006.01.021

Slama, M. C., Ravicz, M. E., & Rosowski, J. J. (2010). Middle ear function and cochlear input impedance in chinchilla. *The Journal of the Acoustical Society of America*, *127*(3), 1397-1410. https://doi.org/10.1121/1.3279830

Smith, C. W., Young, I. S., & Kearney, J. N. (1996). Mechanical properties of tendons: Changes with sterilization and preservation. *Journal of Biomechanical Engineering*, *118*(1), 56-61. https://doi.org/10.1115/1.2795946

Soldevilla, M. S., McKenna, M. F., Wiggins, S. M., Shadwick, R. E., Cranford, T. W., & Hildebrand, J. A. (2005). Cuvier's beaked whale (*Ziphius cavirostris*) head tissues: Physical properties and CT imaging. *Journal of Experimental Biology*, *208*(12), 2319-2332. https://doi.org/10.1242/jeb.01624

Soons, J. A., Aernouts, J., & Dirckx, J. J. (2010). Elasticity modulus of rabbit middle ear ossicles determined by a novel micro-indentation technique. *Hearing Research*, *263*(1-2), 33-37. https://doi.org/10.1016/j.heares.2009.10.001

Speirs, A. D., Hotz, M. A., Oxland, T. R., Häusler, R., & Nolte, L. P. (1999). Biomechanical properties of sterilized human

auditory ossicles. *Journal of Biomechanics*, *32*(5), 485-491. https://doi.org/10.1016/S0021-9290(99)00012-3

Stäubli, H. U., Schatzmann, L., Brunner, P., Rincón, L., & Nolte, L. P. (1999). Mechanical tensile properties of the quadriceps tendon and patellar ligament in young adults. *The American Journal of Sports Medicine*, *27*(1), 27-34. https://doi.org/10.1177/03635465990270011301

Thorpe, C. T., Riley, G. P., Birch, H. L., Clegg, P. D., & Screen, H. R. (2014). Effect of fatigue loading on structure and functional behaviour of fascicles from energy-storing tendons. *Acta Biomaterialia*, *10*(7), 3217-3224. https://doi.org/10.1016/j.actbio.2014.04.008

Thorpe, C. T., Klemt, C., Riley, G. P., Birch, H. L., Clegg, P. D., & Screen, H. R. (2013). Helical substructures in energy-storing tendons provide a possible mechanism for efficient energy storage and return. *Acta Biomaterialia*, *9*(8), 7948-7956. https://doi.org/10.1016/j.actbio.2013.05.004

Tubelli, A. A., Zosuls, A., Ketten, D. R., & Mountain, D. C. (2014). Elastic modulus of cetacean auditory ossicles. *The Anatomical Record*, *297*(5), 892-900. https://doi.org/10.1002/ar.22896

Tubelli, A. A., Zosuls, A., Ketten, D. R., & Mountain, D. C. (2018). A model and experimental approach to the middle ear transfer function related to hearing in the humpback whale (*Megaptera novaeangliae*). *The Journal of the Acoustical Society of America*, *144*(2), 525-535. https://doi.org/10.1121/1.5048421

Tubelli, A. A., Zosuls, A., Ketten, D. R., Yamato, M., & Mountain, D. C. (2012). A prediction of the minke whale (*Balaenoptera acutorostrata*) middle-ear transfer function. *The Journal of the Acoustical Society of America*, *132*(5), 3263-3272. https://doi.org/10.1121/1.4756950

Tuck-Lee, J. P., Pinsky, P. M., Steele, C. R., & Puria, S. (2008). Finite element modeling of acousto-mechanical coupling in the cat middle ear. *The Journal of the Acoustical Society of America*, *124*(1), 348-362. https://doi.org/10.1121/1.2912438

Vergari, C., Pourcelot, P., Holden, L., Ravary-Plumioën, B., Gerard, G., Laugier, P., . . . Crevier-Denoix, N. (2011). True stress and Poisson's ratio of tendons during loading. *Journal of Biomechanics*, *44*(4), 719-724. https://doi.org/10.1016/j.jbiomech.2010.10.038

Wahlberg, M., Delgado-García, L., & Kristensen, J. H. (2017). Precocious hearing in harbour porpoise neonates. *Journal of Comparative Physiology A*, *203*(2), 121-132. https://doi.org/10.1007/s00359-017-1145-0

Wang, X., & Gan, R. Z. (2016). 3D finite element model of the chinchilla ear for characterizing middle ear functions. *Biomechanics and Modeling in Mechanobiology*, *15*(5), 1263-1277. https://doi.org/10.1007/s10237-016-0758-5

Wartzok, D., & Ketten, D. R. (1999). Marine mammal sensory systems. In J. E. Reynolds III & S. A. Rommel (Eds.), *Biology of marine mammals* (pp. 117-175). Washington, DC: Smithsonian Institution Press.

Willi, U. B., Ferrazzini, M. A., & Huber, A. M. (2002). The incudo-malleolar joint and sound transmission losses. *Hearing Research*, *174*(1-2), 32-44. https://doi.org/10.1016/S0378-5955(02)00632-9

Woo, S. L. Y., Orlando, C. A., Camp, J. F., & Akeson, W. H. (1986). Effects of postmortem storage by freezing on ligament tensile behavior. *Journal of Biomechanics*, *19*(5), 399-404. https://doi.org/10.1016/0021-9290(86)90016-3

Yamato, M., Ketten, D. R., Arruda, J., Cramer, S., & Moore, K. (2012). The auditory anatomy of the minke whale (*Balaenoptera acutorostrata*): A potential fatty sound reception pathway in a baleen whale. *The Anatomical Record*, *295*(6), 991-998. https://doi.org/10.1002/ar.22459

Zhang, X., & Gan, R. Z. (2013). Dynamic properties of human tympanic membrane based on frequency-temperature superposition. *Annals of Biomedical Engineering*, *41*(1), 205-214. https://doi.org/10.1007/s10439-012-0624-2

Zioupos, P. (2005). In vivo fatigue microcracks in human bone: Material properties of the surrounding bone matrix. *European Journal of Morphology*, *42*(1-2), 31-42. https://doi.org/10.1080/09243860500095463

Zioupos, P., Currey, J. D., & Casinos, A. (2000). Exploring the effects of hypermineralisation in bone tissue by using an extreme biological example. *Connective Tissue Research*, *41*(3), 229-248. https://doi.org/10.3109/03008200009005292